Available online at www.sciencedirect.com

SciVerse ScienceDirect

Procedia CIRP 9 (2013) 49 – 54

www.elsevier.com/locate/procedia

2nd CIRP Global Web Conference

# Efficient Spatial and Temporal Modelling of Material Temperatures Within Self-Reinforced Polypropylene Sheets During IR Radiation

Stefan Hess[a,]*, Angela Ries[b], Petra Kersting[a], Hans-Peter Heim[b]

[a]*Institut of Machining Technology, TU Dortmund University, Baroper Str. 301, 44227 Dortmund, Germany*
[b]*Institute for Materials Engineering, University of Kassel, Mönchebergstr. 3, 34125 Kassel, Germany*
** Corresponding author. Tel.: +49-231-755-2364; fax: +49-231-755-5141.E-mail address: hess@isf.de.*

**Abstract**

Polymer composites of self-reinforced fibres and a matrix composed of the same plastic material display an outstanding mechanical performance and an excellent recyclability. Hence, these materials are suitable for many practical applications. One disadvantage, however, is the narrow processing window that is caused by a strong pressure and temperature sensitivity of the self-reinforced fibres. In this paper, an approach to efficiently model the spatial and temporal temperature evolution is presented. Advanced empirical modelling techniques from the design and analysis of computer experiments are fitted to experimental data. It is shown that only a small set of experiments has to be performed in order to predict the temperatures with the desired accuracy. The required enhancements with respect to the design of experiments and the empirical models are presented.



*Keywords:* Polymers; Empirical Modelling; DACE Models; Kriging; IR Radiation; Self-Reinforced Polypropylene; Textile Sheets

## 1. Introduction

The principle of self-reinforced thermoplastic composites bases on an intrinsic orientation of the macromolecules in the component. The self-reinforcement thereby strongly improves the mechanical properties in longitudinal fibre direction without implementing additional reinforcement (e. g. fibres). These outstanding properties concern among others higher stiffness and strength. This enables an excellent recyclability and suitability for many practical applications, like flexible hinge-joints, crash absorber pads with high impact resistance, as well as screwing points with high local stiffness properties to prevent creeping [1]. Industrial applications are for instance automotive parts (door and undertray), shinguards and loudspeaker cones [2]. Besides the many advantages of self-reinforced polypropylene composites, the manufacturing process is a challenging task. The materials are very sensitive to variations of pressure and temperature. Also, the impact of the input parameters on the desired properties is highly nonlinear. In order to control the entire process chain, a precise knowledge of the input-output relationship in every process is crucial. This includes the pre-heating of the materials, where a precise control of the temperature distribution throughout the component volume is indispensable. Due to the lack of material models and the combination of solid and fluid elements due to partial melting and air between the layers of the uncompacted composite, the use of finite element methods is not an efficient option with respect to the number of experiments for calibrating the parameters and the time required for evaluation. Empirical approximation models, often called surrogate models or meta-models, are excellent solutions to surmount this challenge [3,4,5]. Standard regression models, however, often fail to describe the highly nonlinear relationship between input and output parameters. The required enhancements are provided by design and analysis of computer experiments (DACE).


doi:10.1016/j.procir.2013.06.167

Wagner et al. [5] pointed out that DACE models are an excellent choice to represent the gradient properties of polypropylene (PP) sheets in a hot-compaction process. These models are distinguished by the fact that they can depict complex nonlinear relationships. They could, therefore, carry out a multi-objective optimization of the graded properties of PP composites in their work. One conclusion from this study was that the properties are not only dependent on input factors, such as pressing temperature and pressure, but also on the initial material temperature. However, in their experiments, the material temperature was only measured by five sensors placed diagonally on the component surface. Therefore, the information about the evolution of the material temperature in the prior pre-heating process is still very vague. This work aims to fill this information gap. By means of a precise modelling of the temperature distribution of the component volume, the entire process chain can therefore be refined.

## 2. Self-Reinforced Polypropylene Composites

### *2.1. Material and composite properties*

The self-reinforcement of polypropylene is based on a melt and solid phase deformation of the polymer, which leads to exceptional properties [6]. The semi-finished products employed in the experiments are compared in Table 1. For the transfer of the orientation to structural components, an intermediate step becomes necessary. The self-reinforced tape fabrics or fibre fleeces made of polypropylene are layered, preheated and hot compacted to layered composites. Subsequently, they are cooled to fix their orientation.

Table 1. Applied textiles for the pre-heating experiments

| Material System | Class / Colour | Density | Area weight | Numbers of Layers |
|---|---|---|---|---|
| - | - | [g/cm²] | [g/m²] | - |
| Pure | Co-extruded tape fabric / white | 0.760 | 105 | 16 |
| SG30/30 | Mono-extruded tape fabric / black | 0.909 | 124 | 16 |
| SNW17 | Needle-punched fleece / white | 0.930 | 150 | 12 |

On the one hand, the self-reinforcement of the tapes and fibres must be preserved throughout this processing, in order to maintain the excellent properties [2]. On the other hand, the material must be melted partially to generate a sufficient matrix phase for the embedding of the tapes or fibres. These conditions are necessary to fulfil the outstanding composite properties and if a successful compromise of both effects can be achieved, self-reinforced polypropylene composites are five times higher with regards to stiffness and strength in comparison to polypropylene components manufactured by injection moulding or extrusion [1]. In the context of this investigation, three different textile products were chosen; compare Fig. 1 and Table 1. On one hand a special for composite manufacturing modified co-extruded tape fabric named Pure by Lankhorst, Netherlands was applied. Further information about the material properties, like mechanical properties and thermal stability can be found in [1,7]. On the other hand two geotextiles from Bonar, Belgium were used. This includes a mono-extruded twill weave with the labeling SG30/30 and a needle-punched staple fibre fleece named SNW17.

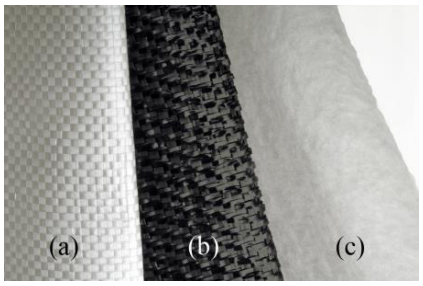


Fig. 1. Polypropylene based semi-finished textile products:
(a) Pure: plain weave; (b) SG30/30: twill weave; (c) SNW 17: needle-punched stable fibre fleece

### *2.2. Manufacturing process*

The considered process chain is shown in Fig. 2. Due to the before mentioned compromise, the ideal processing window is comparably small. The especially high temperature (and thus inevitably time dependent) as well as pressure sensitivity strongly influence the prevalent self-reinforcement, which is to be maintained to a high degree throughout processing and later transferred onto the composite.

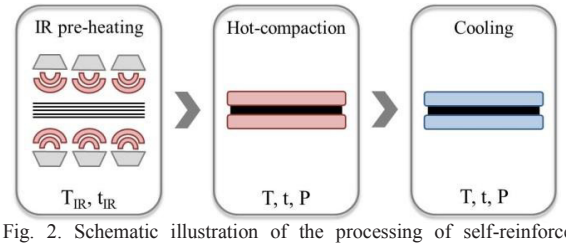


Fig. 2. Schematic illustration of the processing of self-reinforced polypropylene composites.

The pre-heating process allows the layered, semi-finished textile products to be pretempered, making it possible to noticeably reduce the thermal strain subsequently introduced in the consolidation process.

### 2.3. Thermal Gradation during Pre-heating

The component properties can be controlled by means of a thermal gradation introduced in the pre-heating process [1]. To accomplish this, inexpensive, but also very effective masking plates are locally placed between the radiator fields and the textiles (Fig. 3). This is done to significantly decrease the material temperature of pre-heating textile layers. Thus, a differential material temperature is set in the textiles that will ultimately affect the later composite properties.

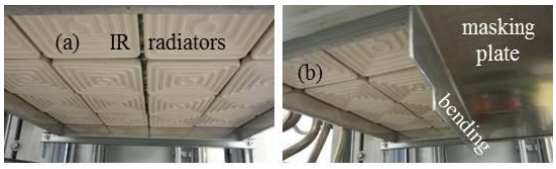


Fig. 3. Used IR pre-heating station without (a) and with (b) masking plates

## 3. Modelling

### 3.1. Formalization of the process

Although pre-heating can be considered as one single process, it needs to be subdivided into consecutive parts for the empirical modelling. First, the temperature of each sensor is modelled. The input factors are heating time $t_H$ and heating temperature $T_H$. The output is the sensor Temperature $T_{Sx}$ of the 22 sensors $S_1,\ldots, S_{22}$. The goal is to predict the temperature in the local areas of the material at any time and at any temperature in the process window. This comprises that a prediction can be made even for input values that were not measured.

Based on the local temperature, the next step is to model the temperature within the component volume. This requires an appropriate distribution of the sensors between the PP textile sheets. The placement of the sensors will be discussed in section 3.4. Furthermore, the masking time $t_M$ can then be included as an input factor by modelling the temperature of the sensors covered by the masking plate. Fig. 4 shows the scheme of how the subdivided process procedure is constructed for empirical modelling.

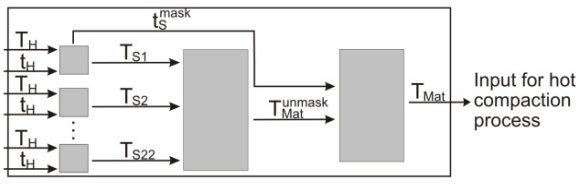


Fig. 4. Scheme of the subdivision of the process for empirical modelling

### 3.2. Surrogate modelling

Surrogate models approximate the functional relationship between input and output parameters of complex nonlinear systems, especially when evaluations of the system are expensive and/or time-consuming. The most popular surrogate modelling approach is polynomial regression [3]. A set of n observation with d input variables $X = (x_1,..., x_d)$ is created by methods of design of experiments. The evaluation of the design leads to n observation pairs $(X^{(i)}, y^{(i)}), i = 1,..., n$ of input parameters and corresponding response values. Polynomial regression models assume the functional relationship $y(X) = f(X) + \varepsilon$ , where the vector of residuals $\varepsilon$ is assumed to be a random noise variable with mean zero and an unknown standard deviation $\sigma$; $f$ is a predefined (usually quadratic) functional term of the input parameters. Polynomial regression models are very efficient when the actual problem function is linear or quadratic [3]. However, it has major drawbacks regarding highly nonlinear problems [5]. This can be indicated by a systematic trend of the residuals, which will be shown in the results section.

Models from the Design and Analysis of Computer Experiments [8], also called Kriging or Gaussian process models, enhance the polynomial regression model by

$$y(X) = f(X) + Z(X), \quad (1)$$

where $f(X)$ is usually a constant term $\beta_0$ or a first order polynomial with a (known) linear trend. $Z(X)$ is a Gaussian process with mean zero and a covariance function $\mathrm{cov}(Z(X^{(i)}), Z(X^{(j)})) = \sigma R$ , where $R$ is a correlation function, which has to be chosen in advance. In this paper, the most general approach by Sacks et al. [8] is used:

$$R(X^{(i)}, X^{(k)}, \theta, p) = \exp(-\sum_{j=1}^{d} \theta_j \left| x_j^{(i)} - x_j^{(k)} \right|^{p_j}) \quad (2)$$

In their original form, DACE models interpolate the empirical data. However, if the problem is assumed to be nondeterministic, this can be represented by a so-called nugget effect [9]. Biermann et al. [10] proved the applicability of DACE models for noisy experiments.

### 3.3. Placement of the Sensors

DACE models require a special experimental design in which the observations are distributed uniformly in the design space. Therefore, the 22 sensors have to be spatially distributed in the three-dimensional design space defined by the x-axis, the y-axis and the textile layers of the latter PP composites. The sensors can be continuously placed between 0 mm and 500 mm on both

axes for all materials. The number of layers has differed, because of thickness differences in the materials. 16 layers were used for Pure and SG30/30. Only 12 layers were used for the thicker SNW17. The location of the sensors was then determined by a Latin Hypercube Sampling [11]. In this context, an assumption could be made which improved the data base considerably. As the component is uniformly heated from both sides, a suitable symmetry can be assumed. Therefore, any sensor can be reflected on the centre of the three axes, resulting in a dense space filling distribution of the sensor information shown in Fig. 5. To ensure the symmetric heating, the temperatures of both IR heating plates were measured continuously during the process.

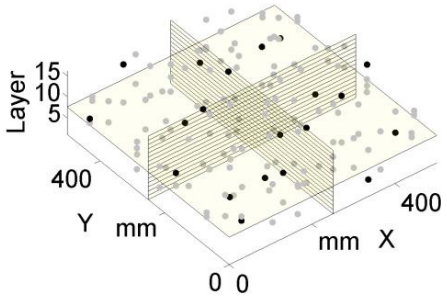


Fig. 5. Distribution of sensors (black) and their reflections (grey) on the centre of the axes

During the experiment two of the sensors showed a temporary failure. These unreliable sensors were completely removed from the data set. Thus, the observations for modelling the component volume were reduced to 20 sensors, i.e., 160 data points in the projected space.

### *3.4. Experimental design*

Designing the experiments for the measurement of the heating temperature, the heating time and the masking time was difficult for several reasons. On the one hand, the heating time should be as long as possible so as to gather a maximum density of information about the material temperature before masking. A maximum heating time in every experiment, however, would introduce an extreme correlation between $T_{IR}$ and the initial material temperature $T_{Mat}$. Therefore, half of the experiments were performed for the maximum heating time of $t_H$=250 s. Another problem was the very limited number of experiments. The material could be heated only a few times, and the preparation by placing and weaving the sensors on the material was arduous work. Therefore, seven parameter settings were the maximum number of experiments for every material. An equidistant spacing was chosen for the heating temperature and the maximum masking time was set to $t_{Mask}$=100 s. The experimental design can be found in Table 2.

Table 2. Experimental Design

| Exp. No | Heating Temp. $T_H$ [°C] | Heating Time $t_H$ [s] | Masking Time $t_{Mask}$ [s] |
|---|---|---|---|
| 1 | 152 | 120 | 100 |
| 2 | 128 | 120 | 100 |
| 3 | 122 | 250 | 100 |
| 4 | 146 | 250 | 100 |
| 5 | 140 | 145 | 100 |
| 6 | 134 | 250 | 100 |
| 7 | 158 | 250 | 100 |

## 4. Results

### *4.1. Empirical modelling of the material temperature*

At first, the temperature at the individual sensors prior to the masking process is modelled. Each temperature of a sensor can be seen as a function of the heating time and heating temperature. Based on the knowledge about the process, some assumptions can be made about the influence of the input parameters on the response. Both the heating time and the temperature cause a monotonic increase of the sensor temperature. By using a linear trend in formula (1), this feature was included in the DACE model. For comparison, a polynomial regression model with quadratic terms and two way interaction was also fitted to the data. The comparison of both approaches is shown in Fig. 6 for sensor $S_1$. It can be clearly stated that the quadratic model cannot represent the functional relationship between the input and output properly since a systematic error concerning the residuals can be observed. In addition, the model illogically predicts a decreasing temperature with increasing time. This proves once again that model choices should always be questioned and validated either qualitatively by means of resampling techniques (e.g. cross validation, bootstrapping,…) [12], and, if possible, qualitatively by visualizing the data. In contrast, the response surface of the DACE model shows a very good fit of the data. The heating time shows a diminishingly increasing effect on the sensor temperature. The heating temperature appears to have a linear influence. The prediction quality of the model was validated by an adapted cross-validation. It would not make sense to remove individual measurements, because the data for a single time series is dense. For this reason, a complete experiment was removed in each case, and predicted by the model that resulted from the other time series. The prediction quality can be measured by the cross validated coefficient of determination $R^2_{CV}$, which can be between

0 (poor prediction quality) and 1 (perfect prediction quality). The determined $R^2_{CV}$ was never below a value of 0,85, which indicates that the DACE model shows a very good fit, even when fitted based on only six experiments. Considering the computational feasibility which allows more than 1000 predictions per second, an efficient surrogate model was obtained.

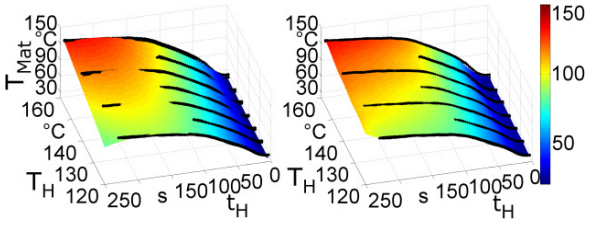


Fig. 6. Resulting response surfaces for both surrogate models: (a) Kriging Model; (b) Polynomial Regression

The key aspect of this paper is the modelling and visualization of the temperature distribution within the component volume. In order to accomplish this, the temperatures of the sensors are also considered as input variables. The temperature of the component volume was modelled using a DACE model. In this case, due to the lack of prior information, $f$ in (1) is a constant term (ordinary Kriging). The predictions of the models provide some interesting insights into the spatial temperature distribution. For instance Fig. 7 compares the modelled temperature progression at a fixed heating temperature of $T_H$=146°C for the different materials.

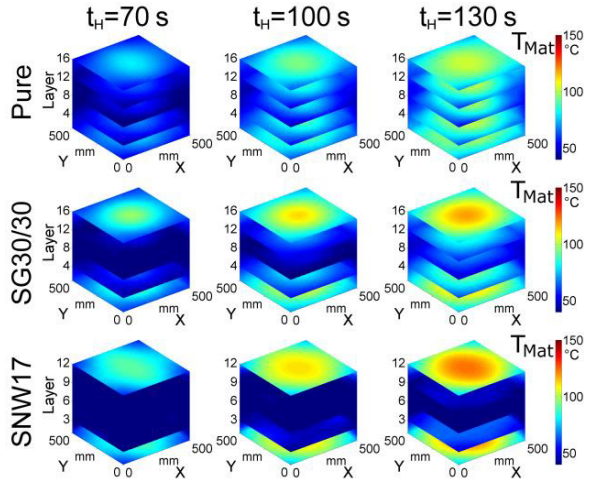


Fig. 7. Temperature distribution of the three materials with $T_H$=146°C

It shows three models with heating times of $t_H$=70 s, 100 s and 130 s. The temperature gradient is clearly visible from the centre to the edge for all materials. In the case of the material Pure it is evident that the applied heat is quickly transported into the inner layers. Thus, the temperature is already distributed uniformly in the material after short heating periods. For SG30/30, only the outer layers show a significant increase of material temperature after $t_H$=70 s and $t_H$=100 s. An increase in temperature between the inner layers becomes visible after $t_H$=130 s. However, the core temperature is hardly higher than $T_{Mat}$=80°C. SNW17 displays an even more extreme heat impermeability. The outer layers hardly allow the heat energy to be transported into the inner layers. Even after $t_H$=130 s, the temperature of the inner layers is below 50°C. Outer layers have a significantly higher temperature when the material proves to be impermeable to heat. When comparing the three materials after being heated for $t_H$=130 s, the maximum temperatures of the outer layers of SG30/30 (115°C) and SNW17 (125°C) are considerably higher than that of Pure (92°C). This is due to the fact that the heat was conducted into the inner layers relatively quickly in Pure.

Resampling methods are used for validation. According to [13], all DACE models are evaluated by means of a leave-one-out cross-validation. Of course, also the duplicates of each omitted point were omitted as well. Fig. 8 illustrates the comparison of the true and predicted response values for the three materials with $t_H$=130 s and $T_H$=146°C. It can be seen that the overall prediction quality of the model was good, since the points are quite near to the optimal prediction line and no systematic trends in the residuals can be observed. Only in the case of Pure some outliers show discrepancies. Of all 7 Experiments with each material, the median of the cross-validated mean absolute error value was about 5,5°C, which can be regarded as a good prediction quality.

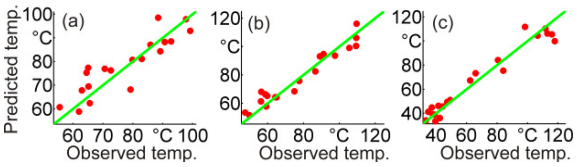


Fig. 8. Plot of observed vs. predicted temperatures of the sensors after cross validation for (a) Pure; (b) SG30/30; (c) SNW17

Last, the masking phase must be described by empirical models. Therefore, the sensor temperature before masking and the masking time are used as the input parameter for the masked sensors. Here, the symmetry assumption must be restricted. The reflection on the y-axis has to be skipped due to the local effect of the masking.

Fig. 9 depicts the material temperatures measured for the three materials after $t_H$=250 s heating time and $t_{Mask}$=100 s masking time at a heating temperature of

$T_H$=146°C. The relocation of the hot spot on the y-axis is clearly visible. Due to the long heating time, the temperatures on the surfaces of all materials are approximately the same. Moreover, the heat has reached the inner layers of SG30/30 and SNW17.

It can be concluded that a consistent heat distribution can be achieved quickly for the fabric materials Pure and SG30/30. If a gradation of the temperature between the layers is desired, a very short heating time should be considered. For needle-punched fleece system SNW17 should be taken into account that due to the heat impermeability of the material, even with a short heating time a temperature gradation can be archived. This acquired knowledge can now be used to further understand and control the functional gradation of the composites within the entire process chain.

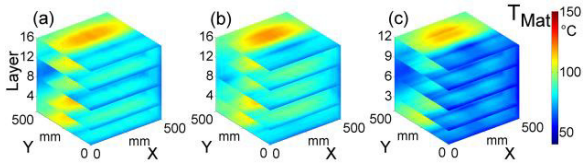


Fig. 9. Temperature distribution with $T_H$=146°C and $t_H$=250 s after a masking time of $t_{Mask}$=100 s for (a) Pure; (b) SG30/30; (c) SNW17

## 5. Summary

In this paper, a sophisticated approach to efficiently model the spatial and temporal temperature evolution was presented. The model formalization was subdivided into different submodels. First, the temperature was modelled using 22 sensors that were woven into the layers of a PP composite. A DACE model with a linear trend, which takes the monotonic influence into account, was employed for the input parameters heating time and heating temperature. It was shown that conventional methods like polynomial regression are not able to fully describe the functional relationship between input and output parameters. In the following modelling step, the temperatures of the individual sensors were used to predict the temperature distribution within the component volume. By integrating symmetry assumptions, the data base could be significantly improved. The modelling provided some interesting insights concerning the different spatial temperature progressions of the three materials Pure, SG30/30 and SNW17. These models were thoroughly validated using qualitative and quantitative methods. They provided a good match of the true and predicted temperatures.

Using the empirical models of the pre-heating process, a sufficiently precise evaluation of the system can be made without having to perform further real experiments. This is especially helpful for a backwards optimization of the process chain for given specifications of the graded properties. Furthermore, the surrogate models enable a profound sensitivity analysis and refining of the knowledge acquired about the propagation of uncertainty in the entire process chain [14].

## Acknowledgements

This paper is based on investigations of the projects D5 and A5 of the Collaborative Research Center SFB/TR TRR 30, which is kindly supported by the Deutsche Forschungsgemeinschaft (DFG).

## References

[1] Bledzki, A.K., Heim, H.-P., Paßmann, D., Ries, A., 2012. Manufacturing of Self-Reinforced All-PP Composites, in *"Synthetic Polymer-Polymer Composites"* D. Bhattacharyya, F. Stoyko, Editor. Carl Hanser Verlag, Munich, pp. 719-738.

[2] Ward, I.M., Hine, P.J., 2004. The science and technology of hot-compaction, Polymer 45, pp. 1413-1427

[3] Montgomery, D.C., 1997. Design and Analysis of Experiments, 4th ed.. John Wiley and Sons, New York.

[4] Wang, G.G., Shan, S., 2007. Review of Metamodeling Techniques in Support of Engineering Design Optimization, Journal of Mechanical Design 129(4), pp. 370-380.

[5] Wagner, T.; Passmann, D.; Weinert, K.; Biermann, D.; Bledzki, A. K., 2008. „Efficient Modeling and Optimization of the Property Gradation of Self-Reinforced Polypropylene Sheets Within a Thermo-Mechanical Compaction Process", 6th CIRP Int'l Conf. Intelligent Comp. in Manufacturing Engineering (ICME 2008)

[6] Heim, H.P., Rohde, B., Ries, A., 2012. "Influence of the Process conditions on the Morphology-Property-Relationship of Self-Reinforced PP-Composites", 1st Int'l Conf. Thermo-Mechanically Graded Materials, Kassel, Germany

[7] Alcock, B., Cabrera, N. O., Barkoula, N. M., Peijs, T., 2009. The Effect of Processing Conditions on the Mechanical Properties and Thermal Stability of Highly Oriented PP Tapes. European Polymer Journal, 45(10), pp. 2878-2894.

[8] Sacks, J., Welch, W.J., Mitchell, T.J., Wynn, H.P, 1989. Design and Analysis of Computer Experiments, Statistical Science, 4(4), pp. 409-435.

[9] Cressie, N.A.C., 1993. Statistics for Spatial Data (revised ed.). Wiley, New York.

[10] Biermann, D., Weinert, K., Wagner, T., 2008. "Modelbased Optimization Revisited: Towards Real-World Processes", IEEE Congress on Evolutionary Comp. 2008. Hong Kong.

[11] McKay M.D., Conover W.J., Beckman R.J., 1979. A comparison of three methods for selecting values of input variables in the analysis of output from a computer code, Technometrics 21, pp. 239–245.

[12] Bischl, B., Mersmann, O., Trautmann, H., Weihs, C. 1012. Resampling Methods for Meta-Model Validation with Recommendations for Evolutionary Computation, Evolutionary Comp. 20(2), pp. 249-275.

[13] Jones, D.R., Schonlau, M., Welch, W.J., 1998. Efficient Global Optimization of Expensive Black Black-Box Functions, Global Optimization 13(4), pp. 455-492.

[14] Biermann, D., Gausemeier, J., Heim, H.P., Hess, S., Petersen, M., Ries, A., Wagner, T., 2012. „Computer-Aided Planning and Optimization of Manufacturing Processes for Functional Graded Components", 1st Int'l Conf. Thermo-Mechanically Graded Materials, Kassel, Germany